

ADAPTIVE UTILIZATION OF PRESSURE SENSOR DATA IN EXCAVATION

Hannu Juola, Rauno Heikkilä, Matti Immonen and Ilpo Niskanen

Addresses Oulu University, Faculty of Technology, Civil Engineering Research Unit, P.O.Box 4200, FI-90014 Oulu, Finland

E-Mail hannu.juola@oulu.fi

Highlights

- Adaptive utilization of pressure sensor data
- Soil boundary detection through correlation
- Effects of torque range limitations on correlation results
- Uses and potential limitations of pressure sensor correlation

Abstract

The assessment of soil parameters in construction holds significant importance for refining building information modeling (BIM). Our study aimed to investigate the adaptive utilization of pressure sensor data as a dynamic and computationally efficient tool for this purpose. The results reveal a significant correlation between the pressure sensor readings of the hydraulic cylinder in the excavator bucket and the total load during static-dynamic penetration tests conducted in both homogeneous and heterogeneous soil. This correlation holds true across a 100% range of torque, with values recorded at 0.60 and 0.93, respectively. A key strength of this methodology lies in that it enables near real-time detection of verified boundary levels. This feature streamlines the adoption and development of BIM-based excavation methods that seamlessly align with current practical conditions.

Keywords soil boundary, detection, hydraulic pressure, static-dynamic penetration test, correlation, model-based design, ground investigation

1 Introduction

Enhanced machine designs are imperative to address the growing demands placed on construction equipment, aiming for heightened functionality, productivity, and efficiency [1]. The interaction between excavators and model-based design is developed on machine control modeling, which derives information from soil models. These soil models are built on the initial information gathered from ground investigation methods. They give point-specific knowledge of the ground being investigated. Soil models of an entire construction area are then either interpolated from said points or by using estimation methods calculated to form an educated conclusion of soil conditions.

As the objective of ground investigations is to map and identify soil layers and constitutive soil parameters, the amount of information available for a mapped area dictates the reliability of the information. Complete mappings of a construction area are very rarely made, and if conducted, tools for such are very scarce. The most common method used is non-destructive testing, such as ground-penetrating radar mapping. These methods all are conducted as a pre-construction phase.

Modern determination of soil parameters in automated construction is effectively simulated using finite element method (FE) modeling. A recent study by Guan et al. [2] reviewed the considerable

success achieved by FE modeling but recognized the limitation of soil constitutive models as they are only applicable to limited soil types or stress paths [3]. They additionally identified the need for extensive and complex computations to further develop this information into workable models. As a solution to this problem, Guan et al. [2] created a deep learning (DL) incorporated FE model to solve the limitation issues of FE soil models. This DL incorporation does not resolve the need for extensive computational requirements. The challenge of FE modeling and the complexity of calculations create an information and hardware gap between mathematical modeling capabilities and the needs of implementations in the field, as reviewed by Zhang et al. [4]. These computational requirements limit the adaptive utilization of ground investigation data during construction.

As FE models create viable information for soil parameter detection, to understand the entire ground mapping of a construction site we must recognize that ground conditions are heterogenic. For this, You et al. [5] combined random field models (RFM) with discrete element method (DEM) models to account for the granular particle properties of heterogenic soil. This is an effective tool to examine the mechanical properties of granular soil particles, which considers spatial variability and coefficient variance. As Mak et al. [6] concluded in their study, these DEM models are elaborated from soil–tool interaction. This is a model developed from the original universal earth moving equation first presented in studies by Hettiaratchi and Reece [7], transforming pressure sensor data into force prediction data [8]. DEM modeling can numerically propagate soil parameters but needs large amounts of calculation data (effectively a soil library) to determine the correct parameters.

As mentioned in the study of Ma et al. [9], excavator development is focusing strongly on the aspects of productivity and safety. Development to tackle these challenges is through automation of excavation. The abilities of automation rely strongly on information derived from velocity and pressure sensors. The soft sensors used in the autonomous control of excavators rely on computation and further elaboration of pressure sensor readings. The use of hydraulic pressure in model-based prediction requires further development for workable models and reliable automation.

While contemporary determination of soil parameters in construction is adeptly simulated through discrete element method (DEM) modeling, its effectiveness diminishes when aiming for adaptive information in near real-time applications. The extensive computational requirements of DEM modeling have constrained its practical use. Furthermore, existing research lacks instances where model-based prediction or autonomous excavation is executed solely through the utilization of excavator hydraulic pressure data without additional computations. This paper outlines a method aimed at addressing these challenges.

The aim of our study was to investigate the potential of the adaptive utilization of pressure sensor data in excavation by comparing the correlation between pressure readings of a smart excavator and a soil surveying machine. Essentially, the pressure sensor data comparison is used to find changes in soil layers by verifying the depths of soil boundaries during excavation, creating a verified soil boundary throughout an excavated area. Field tests were conducted to simulate various infrastructure conditions commonly found in Scandinavia. Data collection from our test subject smart excavator was made using current tools and the latest wireless network technology.

Based on the main aim, the following questions were set in our study:

1. What are the variations of correlation between penetration test results and excavator pressure sensor readings
 - a. in heterogeneous soil?
 - b. in homogeneous soil?
2. What are the effects of torque range limitations on the correlation results?

3. What are the effective uses and potential limitations of pressure sensor correlation to penetration test results?

2 Materials and methods

2.1 Smart excavator specifications

The smart excavator used in this study was developed by Oulu University's Civil Engineering Research Unit from a standard Bobcat E85 Compact excavator. It is fully automated and can be operated with four different control methods [10,11,12]. The first is typical manual operation mode, whereby a pilot operates the controls of the excavator from inside the cockpit. All readings from the pressure sensors and G2 inclination sensors can be read and recorded in this mode (see Section 2.2). This was the operation type used in our study. Second, the excavator can be operated with a teach-in method, where the movements of the excavator pilot are recorded and repeated by the excavator. Third is an automated method, where the trajectories of the excavator are generated from a machine control model. Lastly, the excavator can be operated via remote control. Here, using a Ubiquiti antenna, readings from all the outfitted lidars, cameras, and sensors can be obtained over the same local network. Connection can be established locally with Wi-Fi-based Ubiquiti or from further distances by Rajant kinetic mesh or 4G/5G broadband. Rajant kinetic mesh is connected to the network either wirelessly or by wired connection (Fig. 1).

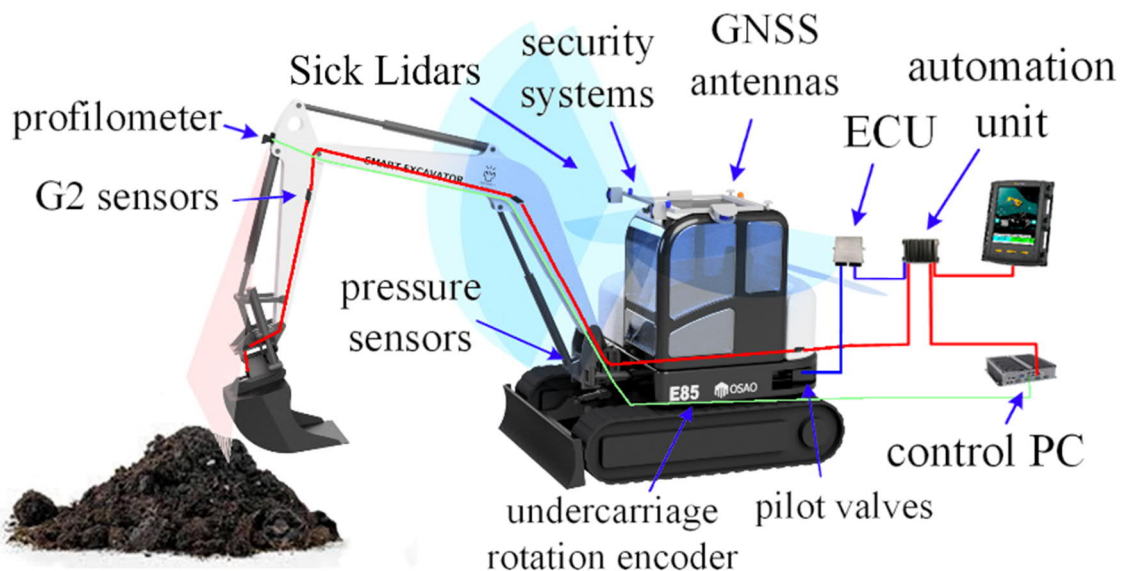


Fig. 1. Layout of the smart excavator used in this study, developed by Oulu University's Civil Engineering Research Unit

2.2 Pressure sensors and data collection

The Oulu University smart excavator was equipped with Gefran KHC pressure transmitters with digital CANopen protocol outputs. These monitor the hydraulic push and pull force parameters of hydraulic pressure from three hydraulic cylinders on the excavator: boom, arm, and bucket. All had monitors for both push and pull force. These transmitters registered the pressure changes during excavation as push force pressure (labeled "A" readings) and pull force pressure (labeled "B" readings).

Signal output of the Gefran pressure transmitters was transmitted via controller area network (CAN) to the motor control center (MCC) and EthCan Kvaser and from here via RJ45 cable to the

ethernet switch and Ubiquiti antenna on the excavator. The pressure readings were then recorded with MATLAB/Simulink on a laptop from the Ubiquiti control booth antenna via RJ45 cable (Fig. 2). Novatron G2 inertial measurement unit (IMU) data were collected parallel to the pressure sensors through the same protocol. This provided the 3D orientation information on the smart excavator needed for the comparison to soundings results of a static-dynamic penetration test (see Section 2.5).

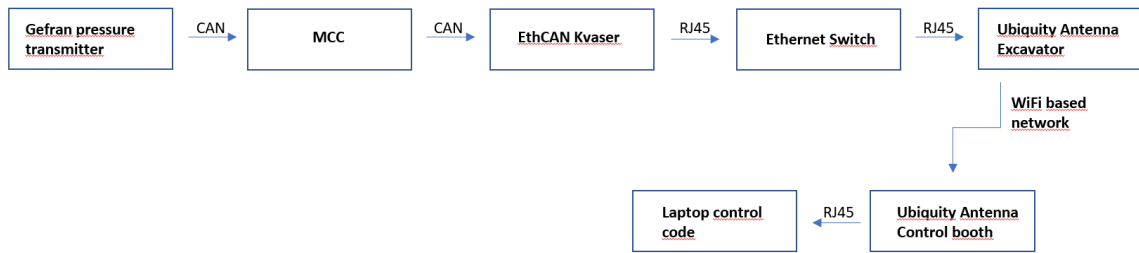


Fig. 2. Signal output sequence of Gefran pressure transmitters

Information from the excavator engine, including RPM and fuel consumption, was recorded via CAN by the EthCan Kvaser CAN USB and transmitted via USB cable to the Beckhoff Industrial PC on the excavator. These readings were downloaded from the Beckhoff Industrial PC to the control booth laptop via Ubiquiti antenna and RJ45 cable (Fig. 3).

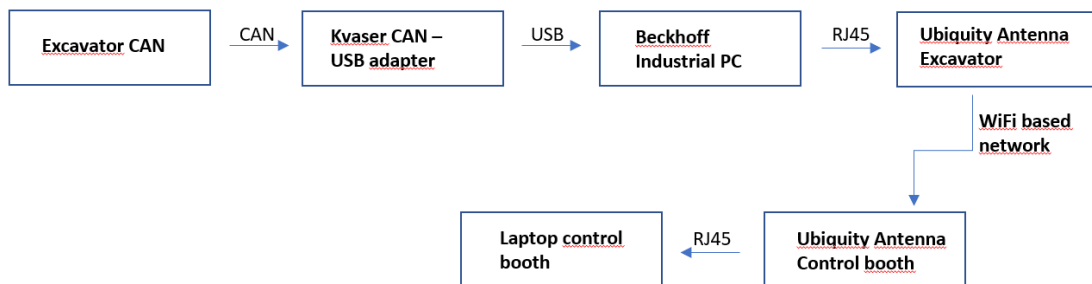


Fig.3. Signal output sequence of excavator engine data

The Gefran KCH pressure transmitter model B04C has a pressure measurement range of 0–400 bar and operates at a 10 msec (1000 Hz) measuring rate. Accuracy at room temperature is $<\pm 0.5\%$ FS. This effects over the compensated range $\pm 0.01\%$ FS/ $^{\circ}\text{C}$ typical ($\pm 0.02\%$ FS/ $^{\circ}\text{C}$ max) [13].

2.3 Data processing and analyses

The data collected from the pressure and G2 IMU sensors during excavation were processed using MATLAB into two separate tables. The data from the pressure sensors were divided into timestamped readings from all three hydraulic cylinders, namely the push and pull force readings from the boom, arm, and bucket. The readings gave a per 10 msec account of the whole excavation. The bucket tip's location with timestamp during excavation can be obtained by using forward kinematics from the recorded IMU data.

From the per 10 msec timestamped location of the excavator bucket's tip, the vertical time stamp z gave the location of the bucket in relation to the ground. From this vertical location data, all readings that were recorded above ground level were discarded. The remaining below ground level location readings were then cross referenced with the timestamped pressure sensor readings, producing a table with excavation pressure readings per 10 msec of each pressure sensor.

From this data, a subtotal average was calculated for each 1 cm of the excavation for all pressure sensor readings (both push and pull forces). This average pressure data was then compared to the static-dynamic penetration test data for the same soil depths.

Excavator engine data, including RPM and fuel consumption, were directly recorded with a timestamp from the ECU to the Beckhoff Industrial PC.

2.4 Study area and soil type

We compared the changes in pressure sensor readings of the smart excavator to the static-dynamic penetration test results when digging in an adhesive soil environment. A set of test pits were dug in two separate locations during November of 2022 and May of 2023. The two test locations represented:

1. homogeneous soil in a sand pit in Jääli, Oulu, Finland.
2. heterogeneous soil in a constructed parking area in Arkala, Oulu, Finland, comprising:
 - a. course layers of crushed rock, 0–56 mm in depth, on top of a fill layer consisting of sandy moraine and large rocks
 - b. moraine subsoil

The Oulu region of Finland has a freezing zone frost protection depth of 1.9 m. At the sand pit site in Jääli, ground water was reached at a depth of 2.9 m below ground level. At the Arkala test site, all test pits were above ground water level. All activities were conducted outside of the freezing period of the year. In both locations, a set of six excavations were conducted with a series of six test pits, respectively. Each series was repeated with the same test pit scheme (Table 1). All test pits were dug at a proximity of < 3 m from the closest static-dynamic penetration test location.

Six static-dynamic penetration tests were conducted to map out the soil condition of a 30 m x 30 m area at each site. These results were then verified with soil samplings (granulation, soil type, and water content) of the same location. This is in line with the ground investigation requirements set by the European Commission's CEN technical committee in NCCI 7.

Table 1. Test pit characteristics of both test areas and individual test pits

<i>Test area</i>					
<i>Heterogeneous soil</i>	<i>Slope</i>	<i>Torque range</i>	<i>Dimensions (l x w x h)</i>	<i>Bucket type</i>	
<i>Test pit</i>	1	1:1.5	100%	2 x 4 x 1.8 m	slope bucket w = 1.5 m, V = 800 l
	2	1:1.5	75%	2 x 4 x 1.8 m	slope bucket w = 1.5 m, V = 800 l
	3	1:1.5	50%	2 x 4 x 1.8 m	slope bucket w = 1.5 m, V = 800 l
	4	1:2	100%	2 x 4 x 1.8 m	trenching bucket w = 0.5 m, V = 400 l

5	1:2	75%	2 x 4 x 1.8 m	trenching bucket w = 0.5 m, V = 400 l
6	1:2	50%	2 x 4 x 1.8 m	trenching bucket w = 0.5 m, V = 400 l

Homogeneous soil

<i>Test pit</i>	1	1:1.5	100%	2 x 4 x 3 m	slope bucket w = 1.5 m, V = 800 l
	2	1:1.5	75%	2 x 4 x 3 m	slope bucket w = 1.5 m, V = 800 l
	3	1:1.5	50%	2 x 4 x 3 m	slope bucket w = 1.5 m, V = 800 l
	4	1:2	100%	2 x 4 x 3 m	trenching bucket w = 0.5 m, V = 400 l
	5	1:2	75%	2 x 4 x 3 m	trenching bucket w = 0.5 m, V = 400 l
	6	1:2	50%	2 x 4 x 3 m	trenching bucket w = 0.5 m, V = 400 l

2.5 Soil parameters and soundings

We limited our test range of soil types to adhesive soil parameters. This decision was made for two reasons. First, we wanted to create a test environment where the studied sensor readings emulated conditions that are represented in a road structure rehabilitation project—a typical example of an infrastructure project. Second, cohesive soil types are not commonly represented in road structures.

Static-dynamic penetration testing was chosen as the comparison to the readings produced by the pressure sensors of the smart excavator. This is a common soundings test administered to map out the condition of the ground's structure. The penetration test in question creates a condition map by combining a cone penetration test with a dynamic probing test. In the cone penetration phase of the test, rods are compressed and rotated simultaneously. In this phase, the compressive force and torque are recorded either with hydraulic pressure or electronically. Compression force is recorded as a total static load of the cone (q_c) at the end of the probing rod (Eq. 1).

$$q_c = \frac{Q_{tot}}{1000 * A_c} \quad (1)$$

where $Q_{tot} = Q_{measured} + Q_{rods}$

q_c = total static load (MPa)

Q_{tot} = total compression force (kN)

A_c = area of penetration cone cross section (m²).

Torque is taken into consideration with net static load q_n (Eq. 2); however, in our case where soundings depth was < 10 m, these are approximately the same ($q_n \approx q_c$):

$$q_n = \frac{Q_{tot}}{1000 * A_c} - k_p * (M_{tot} - \mu_1 - Q_{tot}), \quad (2)$$

where q_n = net static load (MPa)
 Q_{tot} = total compression force (kN)
 k_p = constant ($k_p = 1/A_c * r * 10^6$) = 0.039 (l/m³)
 M_{tot} = total torque (Nm)
 μ_1 = constant made by the soundings riq type (GM-75 = 1 Nm/kN).

The cone penetration test reaches its maximum compressive force at 30 kN, from which the static-dynamic penetration test switches into dynamic probing. Here the rotation of the rod is kept at a steady pace whilst a drop hammer is used on the soundings rod. The result is recorded as net driving amount $N_n/0.2$ m (Eq. 3) [14].

$$N_n = N_{20} - 0.040 * M_{tot}, \quad (3)$$

where N_n = net driving amount
 N_{20} = total driving amount (l/0.2 m)
 M_{tot} = total torque (Nm).

Dynamic probing is changed back to cone penetration when total driving amount drops to < 5/0.2 m. The net driving amounts of dynamic probing can be translated into total static load with Eq. 4:

$$q_c = 0.83 \text{ (MPa/(l/0.2 m))} * N_n. \quad (4)$$

3 Results

3.1 Pressure sensor readings and ground investigation results in heterogeneous soil

The results of the test pit excavations show that pressure sensor readings of the push force pressure in the bucket's hydraulic cylinder correlate with the total static load of the static-dynamic penetration test (Fig. 4 and Table 2). These results were achieved by comparison to slope correlation from multiple test pits with an effective -1.2 m of excavated course layering. In the test pits, first 0.6 m of crushed rock gave a cone penetration reading in total static load until a verified soil boundary depth of -0.60 m below ground. Below the soil boundary, a fill layer consisting of sandy moraine and large rocks was translated from net driving amounts into total static load for a consecutive 0.6m in depth (Eq. 4).

The most accurate correlation was reached with 100% range of torque. With the full range of torque in use, the mean slope of hydraulic pressure correlated with total static pressure to an accuracy of 0.93. A limited 75% range of torque reached 0.71 accuracy in mean slope correlation, and 50% limitation in range of torque was the most inaccurate with 0.68 accuracy (Fig. 4). In general, the mean correlation results improved with the increasing range of torque available; however, there is some overlap in the correlation results to be expected as the fill layer had large

rocks unevenly distributed between the various test pits (Table 2). Standard deviations between the results followed the same trend in result accuracy as the mean slope correlation of each torque range.

The soil boundary level was registered within a 4 cm tolerance of the depth indicated by the static-dynamic penetration test and verified with soil sampling. This tolerance is inside the grain size distribution of the 0–56 mm crushed rock. Both bucket types registered similar readings inside each torque range. The push force pressure in the bucket's hydraulic cylinder was the only pressure reading that gave correlating results. The boom and arm hydraulic cylinders did not register pressure changes that could be accurately compared with the static-dynamic penetration test results. No significant difference was found between the results of excavating a test pit with slope angles of 1:1.5 to the results of slope angles of 1:2.

In general, the cone penetration readings displayed a smaller variation in slope correlation across the measured test pits. Standard deviation increased slightly when excavating in looser soil parameters (Fig. 3). Perhaps the most significant result was discovered in correlation to translated driving amounts, which had a clear increase in accuracy when moving up from smaller driving amounts to denser soil parameters. More specifically, the hydraulic pressure readings of the excavator not only correlated with net driving amount slope changes but were able to be registered per 1 cm of excavated ground. This showed a clear increase as net driving amounts are regularly viewed at 0.2 m intervals.

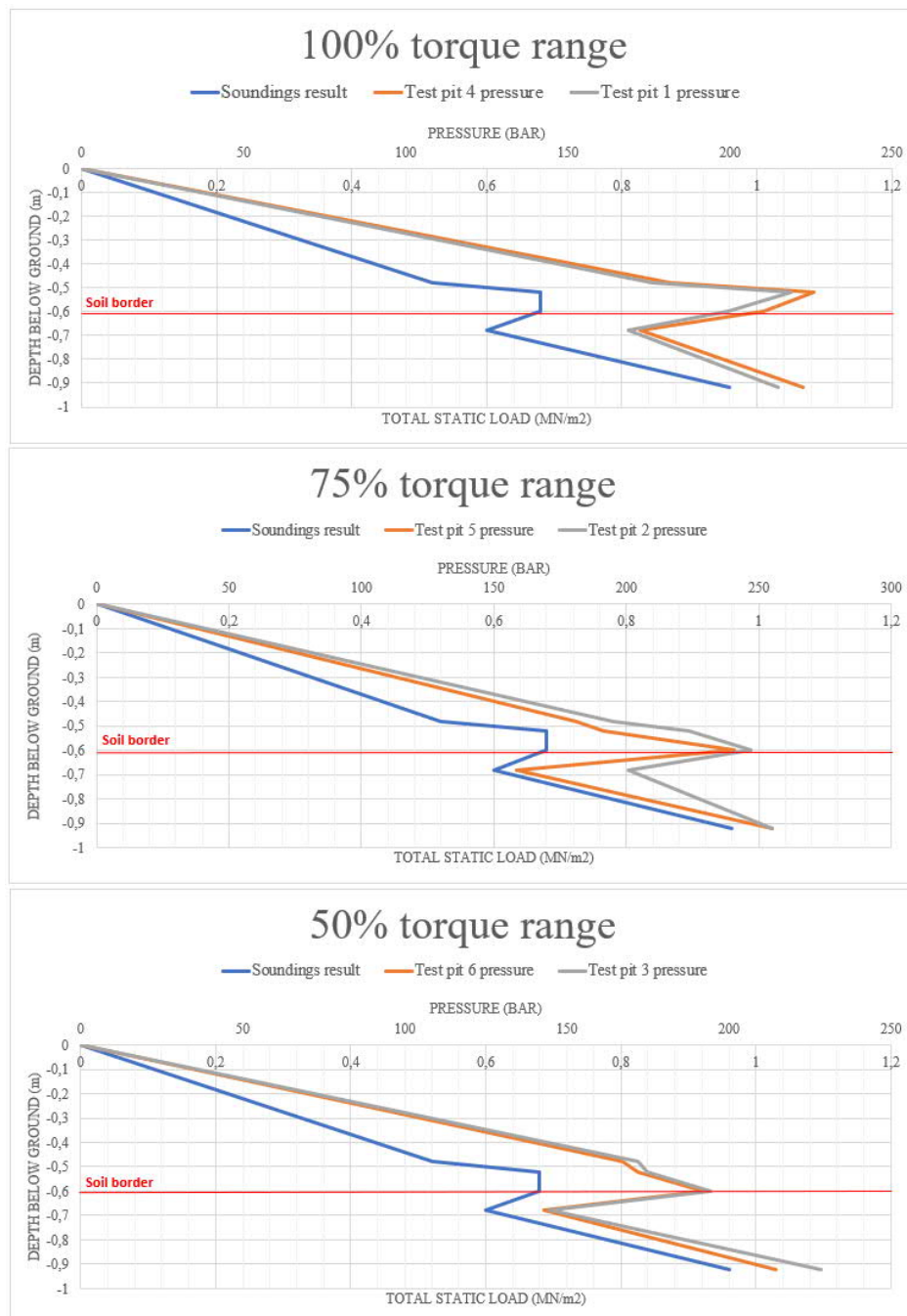


Fig. 4. Correlation results of heterogeneous soil test area per torque limitation range

3.2 Pressure sensor readings and soundings results in homogeneous soil

As with the results in heterogeneous soil, the results of the test pit excavations in homogeneous soil show that the pressure sensor readings of the push force pressure in the bucket's hydraulic cylinder correlate with the total static load of the static-dynamic penetration test. The accuracy follows the same trends on the torque limitations set on the excavator engine as with heterogeneous soil. Here, however, the correlations are not as precise as in heterogeneous soil, where soil boundaries are accurate (Table 2). As homogeneous soil represents layers of different compaction, the changes are more subtle. When viewing the changes in soil compaction in the first 1.8 m of each test pit excavation, the most accurate correlation was reached with the 75% range of torque, where the readings correlated with 0.63 accuracy. The full range of torque reached 0.60 accuracy, and the 50% range of torque was the most inaccurate with 0.57 accuracy (Fig. 5).

Standard deviations between the results followed the same trend in result accuracy as the mean slope correlation of each torque range. As with the results of the heterogeneous soil, standard deviation increased when excavating in looser soil parameters.

It was noted that large variations in compactness within a small distance was not registered with the same correlation as with a static-dynamic penetration test. As an example, a total static load reading of 3.06 MN/m² decreased to 1.86 MN/m² and increased back up to 4.80 MN/m² inside a 36 cm distance in depth. This represents a maximum change in static load of 258.1%. The smart excavator, using the same amount of torque for looser and denser soil, could not react to such quick changes back and forth in such a short distance in depth. The excavator registered this as a 141.7% maximum change in pressure. Only changes into either direction of compactness were registered more precisely. As with heterogeneous soil, these pressure changes were registered within a 4 cm tolerance of the depth indicated by the static-dynamic penetration test. Readings registered below ground water level did not correlate with the static-dynamic penetration test results (Fig. 4).

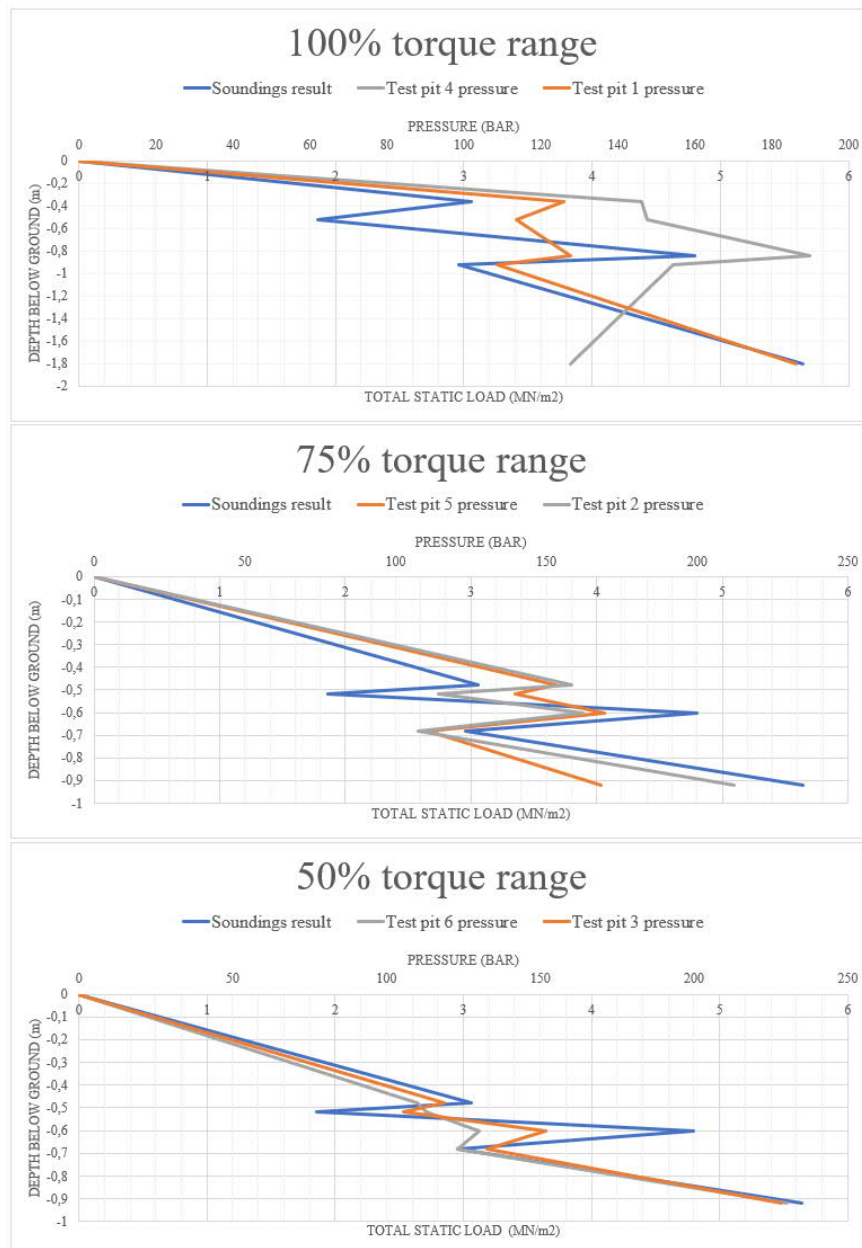


Fig.5. Correlation results of homogeneous soil test area per torque limitation range

Table 2. Correlation of pressure sensors to soundings results

<i>Torque range %</i>	<i>Heterogenous soil Correlation (r)</i>	<i>Homogenous soil Correlation (r)</i>
100	0.93	0.60
75	0.71	0.63
50	0.68	0.57

3.3 Effects of torque range limitation to fuel consumption

During the test pit excavations, fuel consumption was recorded for all three torque ranges. The results of fuel consumption were noted as an isolated feature of the results and therefore are not considered time and production rate changes to the test pit excavations. The results of limiting torque range gave a 9% decrease in fuel consumption from full torque to the 75% limited range. Limiting torque to 50% demonstrated a 22% decrease in fuel consumption from full torque and a 14% decrease from the 75% torque range. No notable difference was recorded between the types of buckets used.

4 Discussion

4.1 Potential and limitations of pressure sensor data in correlation to ground investigations

As the study results demonstrate, excavator pressure sensors can detect soil boundaries in friction soil. The larger the torque range in use, the more accurately the soil borders can be detected using correlation to soundings results. As the compaction varies between soil types, the amount of torque required varies as well. Variance in more subtle compaction levels inside homogenous soil is not as precise. As the effects of torque range limitation clearly affect the amount of fuel consumption, torque range should be limited as much as possible during excavation. With model-based excavation where soil boundary detection is crucial, excavation in homogeneous soil can be executed with torque limitations and full range should be used only when needed or near estimated soil border levels.

Dependable real-time information regarding soil parameters stands as a pivotal factor in construction sites, planning, and decision-making. From an economic perspective, the accuracy of data capture and analysis plays a crucial role in predicting outcomes. The present study demonstrated that the excavator's pressure sensor data can be used in excavation. The study has several important implications. First, utilizing pressure sensor data in soil parameter detection should be focused on distinct borders or constitutive soil parameters in a pre-investigated environment. As the overall accuracy of correlation varies between soil types and densities, this is not a tool for precise ground investigation. The potential of pressure sensor data is in creating a simple and effective tool to verify depths of borders through slope variations in total active pressure. Compared to derived soil-tool models [6,8] where soil parameters [2,15,16,] require prediction of forces and exhaustive estimation calculations, direct comparison of pressure sensor correlation is less exhaustive and site oriented.

A site-specific calibration of soil border correlation between the excavator and ground investigation results is needed for reliable results. The calibration must be repeated per ground investigation point if soil parameters change significantly from one investigation point to another.

The use of pressure data instead of acting forces during excavation cuts down on the amount of estimation and calculations for results. The measurement of forces in an excavation uses the same pressure sensor data but requires additional conversion for reliable outcomes. As the contact forces focused on the bucket are calculated from multiple pressure sensors distributed along boom, arm, and bucket, soil–tool interaction must be considered as well [8]. These are reformulated from Reece’s fundamental earth moving equation [2], adding remolding forces of the payload in the bucket during excavation. The original equations considered excavation on a horizontal plane. This has been developed through estimation tools to a combined method of identification and estimation [2], creating a developed Powell’s tool that accounts for terrain slopes [6]. The latest studies have developed soil parameter detection in soil–tool interactions to utilize finite element methods to model outcomes and parameters. Where estimation through forces supersedes pressure data is in the case of more detailed parameter detections as well as saturated soil interaction. A more detailed study into saturated soil must be made to evaluate the potential of pressure sensor readings.

Total active pressure readings recorded on field computers could be adjusted to record pressure sensor readings of excavators. Translated with current ground investigation software, both pressure readings can be compared in parallel. As our study was limited to friction soils representing common soil types in road structures, more comprehensive field tests are required in the future to test the hypothesis in other prevailing soil conditions.

Additionally, the pressure sensor data produced during an excavation is limited to the amount of pressure that the hydraulic cylinders and pressure sensor models are equipped to withstand. If the soil type requires large forces for excavation, the pressure of the hydraulic cylinder can exceed the threshold of the overflow valves or the maximum capacities in the pressure sensors, creating an imbalance of correlation. This requires that the equipment used for excavation has large enough tolerances for pressure to record all required results.

4.2 Pressure sensor data in future research

Ground investigations give a point-specific account of prevailing soil conditions in a certain area. To create an understanding of the full area in question, the soil boundaries and parameters of investigated points are interpolated to create an estimate of the whole area. As the interpolation is commonly conducted by simply triangulating boundary depths from point to point, the estimation is perfunctory.

A model-based excavation plan for automated excavators using interpolated boundary levels can be developed further if the amount of information fed into the model is dynamic. This can develop a boundary-based excavation model where excavations are conducted to a preset depth or discontinued earlier if a certain boundary is reached. Through such development in soil modeling, we can provide more precise excavations and volume calculations and develop soil models and emission calculations during a project. Developed boundary detection using dynamic information during excavations can allow us to tackle unplanned events during excavation more precisely and in near real-time. The detection of pressure sensor reading correlations with ground investigations could be developed by implementing a detection scheme algorithm, such as the differential detection scheme presented in Tarokh et al. [17], to detect slope changes in penetration test results with site-specific calibration of results to excavator pressure readings.

5 Conclusion

This work proposed a new estimation method for determining soil boundary levels utilizing hydraulic pressure data of excavators. The experimental results indicate that pressure sensor readings of the push force pressure in an excavator bucket hydraulic cylinder correlate with the total

static load of a static-dynamic penetration test. Correlation analysis confirmed the inaccuracy of the pressure data estimation error level of approximately 7%. The main benefits of the method are in the use of pressure data instead of acting forces during excavation, thereby cutting down on the amount of estimation and calculations for results and offering new potential in precise, boundary-based autonomous excavation, the near real-time detection of verified boundary levels and adopting model-based excavation methods with prevailing conditions of practice.

At present, practical challenges for the proposed method include the prevailing conditions and equipment commonly in use. Hydraulic pressure sensors, data collection, and their implementation with model-based design are not commonly in use. Also, the utilization of soundings drilling rig field computers for the recording of excavator pressure data is not common practice.

In future studies, the correlation between hydraulic pressure in excavation and the soundings results of cohesive soil types as well as saturated soils should be studied. Soil boundaries in cut and fill excavations of clay soils are as common as in friction soil.

Acknowledgments

We thank Mr. Samuli Anttila for piloting the Oulu University smart excavator during our field experiments. This study was funded by Business Finland (grant 38056/31/2020) as part of the Open Ecosystem project. The text reflects only the author's views, and the agency is not responsible for any use that may be made of the information it contains.

6 References

- [1] Du, Yu, Dorneich, Michael C. Steward, Brian, - Modeling expertise and adaptability in virtual operator models, *Automation in Construction* 90, 223 -234, 2018, <https://doi.org/10.1016/j.autcon.2018.02.030>
- [2] Q.Z. Guan, Z.X. Yang, N. Guo, Z. Hu, Finite element geotechnical analysis incorporating deep learning-based soil model, *Computers and Geotechnics*, Volume 154, 2023, 105120, ISSN 0266-352X, <https://doi.org/10.1016/j.compgeo.2022.105120>.
- [3] Zhang, P., Yin, ZY., Jin, YF. et al. Modelling the mechanical behaviour of soils using machine learning algorithms with explicit formulations. *Acta Geotech.* 17, 1403–1422 (2022). <https://doi.org/10.1007/s11440-021-01170-4>
- [4] Zhang, P., Yin, ZY. & Jin, YF. State-of-the-Art Review of Machine Learning Applications in Constitutive Modeling of Soils. *Arch Computat Methods Eng* 28, 3661–3686 (2021). <https://doi.org/10.1007/s11831-020-09524-z>
- [5] Minglong You, Changqun Zuo, Fei Tan, Jiahe Lv, Effect of heterogeneity of particle properties on the mechanical properties of sandy soil materials, *Computers and Geotechnics*, Volume 165, 2024, 105890, ISSN 0266-352X, <https://doi.org/10.1016/j.compgeo.2023.105890>.
- [6] Mak, J., Chen, Y., & Sadek, M. (2012). Determining parameters of a discrete element model for soil–tool interaction. *Soil & tillage research*, 118, 117-122. <https://doi.org/10.1016/j.still.2011.10.019>
- [7] Reece, A.R "The Fundamental Equation of Earthmoving Mechanics," *Proceedings of Institution of Mechanical Engineers*, 1964.
- [8] Luengo, O., Singh, S., & Cannon, H. (1998). Modeling and identification of soil-tool interaction in automated excavation. <https://doi.org/10.1109/IROS.1998.724873>
- [9] W. Ma, L. Tan, H. Feng, S. Ma, D. Cao and C. Yin, "A Data-Driven LSTM Soft Sensor Model Based on Bayesian Optimization for Hydraulic Pressure Measurement of Excavator," in *IEEE*

Sensors Journal, vol. 23, no. 21, pp. 25749-25759, 1 Nov.1, 2023, doi:
10.1109/JSEN.2023.3304701.

- [10] Heikkilä, R. & Makkonen, T. & Niskanen, I. & Tyni, P. (2019) Development of an Earthmoving Machinery Autonomous Excavator Development Platform. ISARC 2019, The 36th International Symposium on Automation and Robotics in Construction, Banff, Alberta, Canada, May 21-24, 2019
- [11] Immonen, M. (2014). Ohjaavan 3D-koneohjausjärjestelmän kehittäminen kaivukoneeseen. University of Oulu.
- [12] Mehmood, H., Hiltunen, M., Makkonen, T., Immonen, M., Pirttikangas, S., & Heikkilä, R. (2021) Road map for implementing AI-driven Oulu Smart excavator. International Association for Automation and Robotics in Construction.
- [13] Gefran KHC. (2015), 85206_KHC_User Manual_12-2015_ENG, <http://www.gefran.com>
- [14] Halkola et al. (2001). Kairausopas VI, CPTU/Puristinkairaus Puristin-heijarikairaus, Suomen geoteknillinen yhdistys r.y, <http://www.sgy.fi>
- [15] Gill, W. R., VandenBerg, G. E., Soil Dynamics in Tillage and Traction, Agriculture Handbook No. 316, Agricultural Research Service, US Department of Agriculture, 1968
- [16] Hettiaratchi, D.R.P., Theoretical Soil Mechanics and Implement Design, Soil and Tillage Research, Vol. 11, 1988, pp.325- 347, Elsevier Science Publishers.
- [17] Tarokh, V., & Jafarkhani, H. (2000). A differential detection scheme for transmit diversity. IEEE journal on selected areas in communications, 18(7), 1169-1174. <https://doi.org/10.1109/49.857917>